

Sol gel technique to prepare composite material of glass-dye-polymers

Jayanta K. Ray* and Leena Bhowmik

Department of Chemistry, Indian Institute of Technology, Kharagpur -721302, India

Abstract

Herein we describe the synthesis and in-depth characterization of chemically blended hybrid glasses in which polymer molecules are uniformly distributed and covalently bonded to inorganic matrices. This approach uses a monomer with double bonds, which are hydrosilylated with triethoxy silane and co-condensed with silicon tetraalkoxide to afford a molecular composite of SiO₂ glass and the polymer. The generated coposites were characterized using SEM, TGA and XRD as well as a host of stability tests. They showed increased stability and uniform distribution of the blend.

Introduction

Developments within the area of sol-gel science and technology have led to the proliferation of a vast array of organic-inorganic nano composites. In recent years a large variety of organic and inorganic polymer hybrids have been synthesized by the sol-gel technique utilizing alkoxy silane. A most noticeable characteristic of these hybrid materials is the molecular-level integration of organic and inorganic elements¹⁻³. The interactions that have been utilized to integrate phases are generally classified into two groups, covalent bonding and hydrogen bonding interactions. The covalent interaction is attained by incorporation of silane coupling groups into organic segments. This chemistry can lead to high purity, inorganic, monocomponent and multicomponent glasses. It has led to a class of materials that involves the incorporation of a nanoscopic inorganic phase

into an organic polymer matrix. Polymers and composite materials have thus found applications in various domains⁴⁻²⁸. Sol processing of alkoxy silanes with organic substituents represents a very attractive route to organic-inorganic hybrid materials. The main advantages of sol-gel process are its mild reaction conditions allowing the combination of a large variety of organic monomers with inorganic precursors like tetraethoxy silane and triethoxy silane. The sol-gel process provides inorganic networks or nano particle with polymerizable organic functions. These hybrid materials offer excellent properties as coating materials or as reactive filler compounds in nano composites. We have discussed the preparation and characterization of colored glasses using organic dyes and pigments. But all such composites were cracked after some days. The capillary pressure arising out of evaporation of organic solvents during drying and aging and mainly responsible for the cracks created in the gel glasses. Any manipulation aimed at the decrease of porosity will efficiently reduce the capillary action.

Furthermore, the direct chemical bonding of organic chains to the SiO₂ matrix may help to arrest the cracks, by distribution of the crack propagation energy. This is based on the same mechanism as using the crystal fibers to reinforce the novel ceramic composites. The simultaneous sol-gel condensation of tetraalkoxy silane with polymerizable groups lead to semi-interpenetrating network of linear organic polymer in low density SiO₂ network. The use of the tetraethoxy silane is expected to enhance the incorporation of organic moiety by condensation with terminal O-H group. During the preparation of chemically blended silica glass initially we choose acrylate monomer so that end groups or pendant groups having olefinic function were converted to Si(OEt)₃ by hydrosilylation. Incorporation of organic polymers into inorganic glass matrix via covalent bonding is particularly interesting because the new hybrid material would have a controllable combination of the properties of both organic polymer and inorganic glasses. Many polymers such

as poly (dimethylxysilane), poly (tetra methylene oxide), polyamide, poly (arylene ether ketone) and poly (arylene ether sulfone) were reported to be incorporated into SiO₂ and/or TiO₂ glass network²⁹⁻³². At the current stage, most research is concentrated on the synthesis and tailoring the microstructures of the new hybrid material. There are relatively few reports that explore physical properties and application of this material. A very interesting interpenetrating polyacrylate-SiO₂ composite was prepared recently by simultaneous formation of the SiO₂ sol-gel glass and polyacrylate³³⁻³⁶. We have been interested in the synthesis of chemically blended hybrid glasses in which polymer molecules are uniformly distributed and covalently bonded to inorganic matrices³⁷⁻³⁹. In our approach monomer having double bond are hydrosilylated with triethoxy silane and condensed with silicon tetraalkoxide to afford a molecular composite of SiO₂ glass and the polymer. Inorganic alkoxides are expected to increase the thermal stability of the polymer.

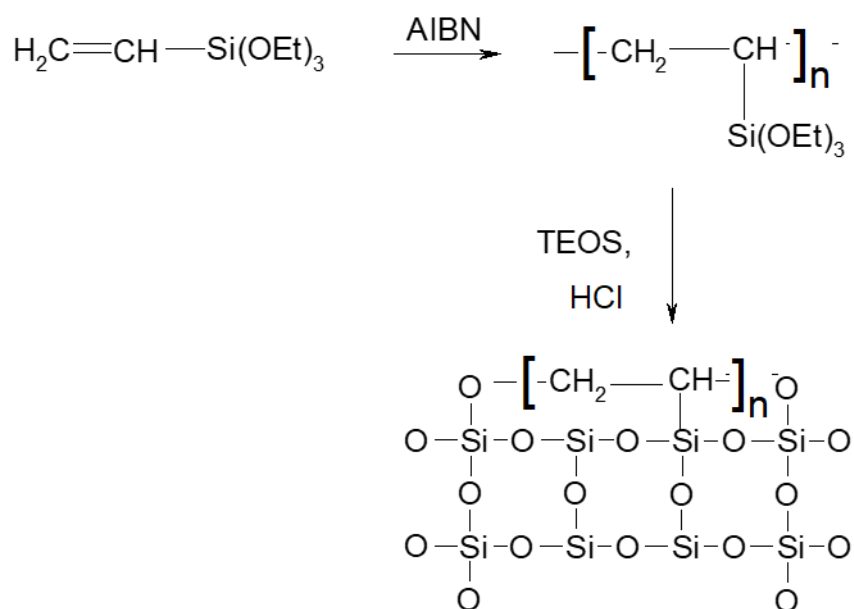
Experimental

Materials

Methyl methacrylate (MMA), Naphthol and vinyl triethoxy silane were purchased from Fluka. Reagent grade triethoxy silane was purchased from Aldrich. Hydrochloric acid, THF and Alizarin were purchased from EMerck. Chloroplatinic acid (H₂PtCl₆) was purchased from Aldrich was purchased from Fluka.

Synthesis of inorganic-organic hybrid sol-gel glass

Monomers having vinyl groups used in this particular work were polymerized via free radical pathway, such as methyl methacrylate, allyl methacrylate, vinyl triethoxysilane. The polymers thus obtained contain end groups or pendants having olifinic functions or trialkoxysilane group respectively. By hydrosilylation, trialkoxysilyl groups were incorporated into the unsaturtated pendants. After this the polymer and tetraethyl orthosilicate (TEOS) were hydrolyzed and condensed by sol-gel technique to produce the chemically bonded hybrid glass. These syntheses are described in different schemes.



Scheme 1 Vinyl triethoxy silane derived sol-gel glass (VNY-SiO₂)

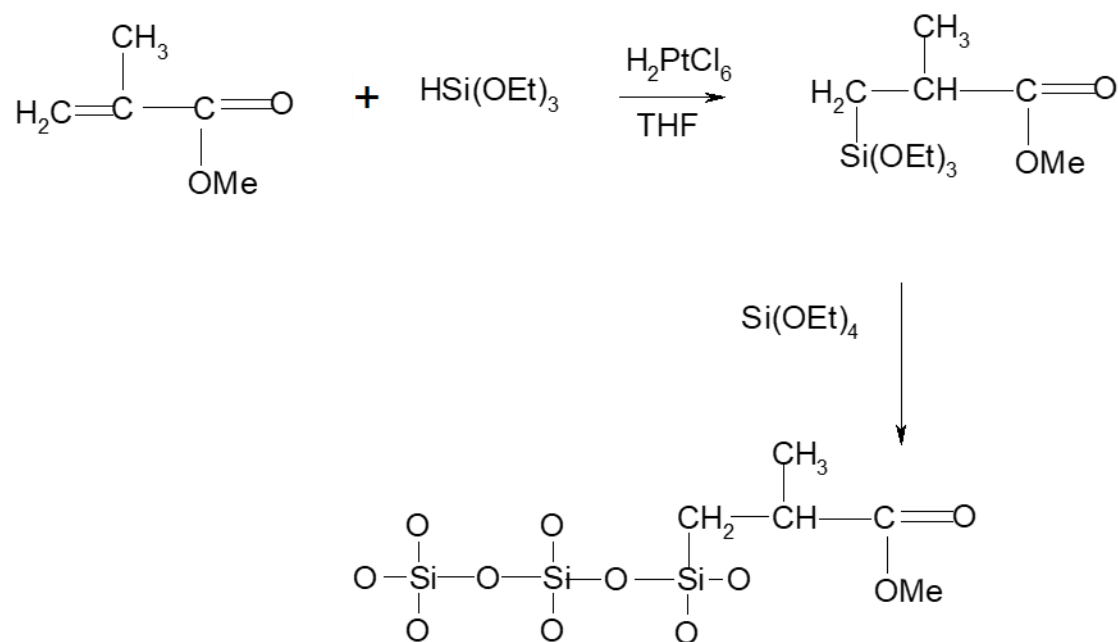
Synthesis of Vinyl triethoxy silane derived sol-gel glass (VNY-SiO₂)

A 50 ml round bottom flask was charged with 4 ml vinyl triethoxy silane which was polymerized using AIBN as initiator at 60 °C temperature. After that the prepared polyvinyl triethoxy silane was taken in a 50 ml round bottom flask and dissolved in anhydrous THF and 2 ml TEOS were added. Then a catalytic amount of 1M HCl and distilled water were added dropwise and stirring

was continued for 24 h. The solution was then poured in a beaker of 4 cm diameter and covered with a paraffin film with holes punched into it. After 30 days a silica glass was obtained.

Synthesis of Methyl methacrylate derived sol-gel glass (MMA-SiO₂)

In a round bottom flask 10 mg of Spier's catalyst (H₂PtCl₆) was dissolved in dry THF under argon atmosphere. After that 1.25 ml of MMA and 2.3 ml of triethoxysilane were added. Stirring was continued at room temperature. After 30 min of stirring black PtO₂ precipitate was separated, which indicated that the completion of reaction. THF was removed by applying vacuum. By column chromatography PtO₂ was removed from final hydrosilylated product. Then the prepared hydrosilylated methyl methacrylate was dissolved in dry THF in a 50 ml round bottom flask. 2 ml TEOS was then added along with a, catalytic amount of 1M HCl and water and the reaction was continued for 24 h. The solution mixture was then poured in a beaker and allowed to stand at room temperature with a perforated paraffin film cover. The glass was obtained after 20 days of drying.

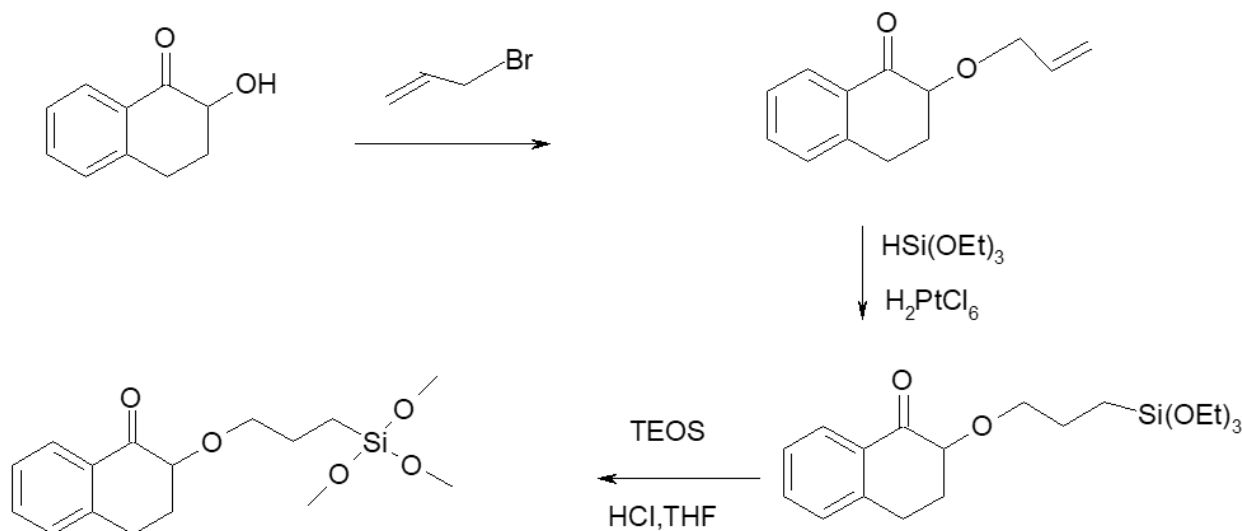


Scheme 2. Synthesis of Methyl methacrylate derived sol-gel glass (MMA-SiO₂)

Preparation of 2-Hydroxy-3,4-dihydro-2Hnaphthalene-1-one derived sol-gel glass (NAP-SiO₂ glass)

0.275g (1.85 m mol) NaI and 0.152 ml allyl bromide were added to 10 ml acetone solution and stirred for 30 min. Then 0.68 g of K₂CO₃ and 0.30 g of reagent were added. The mixture was refluxed in a water bath. After 5 h the reaction mixture was poured into ice-cold water and extracted with diethyl ether. After evaporation of solvent the product was purified by column chromatography.

The allylated product was then hydrosilylated by using Spier's catalyst. 10 mg of Spier's catalyst was dissolved in dry THF solution and argon gas was passed. The solution was stirred for 15 min to dissolve the catalyst. 1 ml of allylated product and 1.5 ml triethoxy silane were added to the contents of the flask by a syringe. The reaction was exothermic. Stirring was continued for 1 h under N₂ atmosphere. After completion of reaction the solvent was removed under reduced pressure. Then 0.5 ml of hydrosilylated naphthalene derivative was dissolved in 10 ml of dry THF. and 2 ml TEOS, catalytic amount of 1M HCl and distilled water were added and stirring was continued overnight. The homogeneous viscous solution was poured in a 50 ml beaker covered with perforated paraffin film and silica glass was obtained after a month.



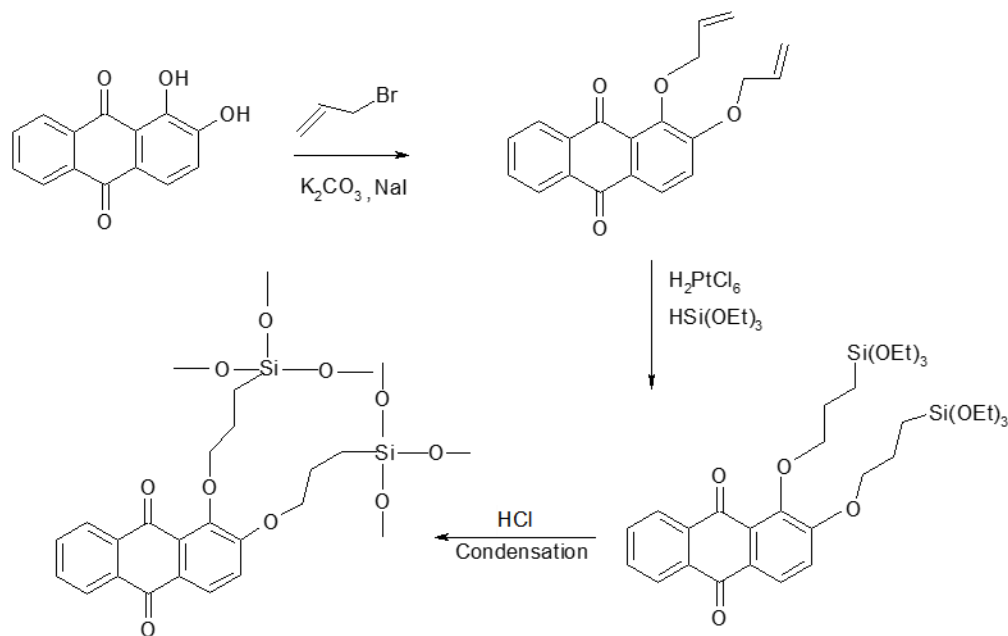
Scheme 3. Synthesis of Hydroxy-3,4-dihydro-2Hnaphthalene-1-one derived sol-gel glass (NAP-SiO₂ glass)

Synthesis of Alizarin derived sol-gel glass (Chem-Ali-SiO₂)

A mixture of 0.52 g (3.0 m mol) of NaI and 0.23 ml of allyl bromide were dissolved in dry acetone in a 10 ml round bottom flask and stirred for 30 min. After that around 1.3 g of K₂CO₃ was added followed by the addition of 0.36 g (1.5 m mol) of alizarin. The mixture was refluxed for 8 h. The reaction mixture was then poured into ice-cold water and extracted with diethyl ether. The yellow solid was obtained after evaporation of solvent and subjected to column chromatography using benzene-petroleum ether. The desired product was obtained as the first elute. The solvent was removed by applying vacuum and dried.

Then 0.40 g bis-O-allyl alizarin (1.25 m mol) was dissolved in 1 ml dry THF. To this solution 0.02 g of H₂PtCl₆ and triethoxy silane were added. Stirring was continued in nitrogen atmosphere for 1 h. After completion of the reaction the solvent was removed *in vacuo*. By column chromatography PtO₂ was removed from the hydrosilylated product.

A 50 ml round-bottomed flask was charged with a solution of bis hydrosilylated alizarin in THF. Then 2 ml of TEOS was added and stirred at room temperature. Required amount of HCl and distilled water were added, and the reaction was continued for 24 h. The solution was then poured in a beaker and allowed to stand at room temperature with a perforated paraffin film cover. The glass was obtained after few days of drying.



Scheme 4. Synthesis of Alizarin derived sol-gel glass (Chem-Ali-SiO₂)

FTIR and NMR spectroscopic analysis

Infrared absorption spectra were recorded between 400- 4000 cm⁻¹ by Fourier transform infrared spectrophotometer (FTIR) (Perkin-Elmer).

Thermal stability

Thermal analysis (TG-DTA) of the silica composite was done on a Shimadzu DT-40 unit, under N₂ atmosphere. A heating rate of 10⁰C min⁻¹ was used.

Scanning electron microscopic analysis

Scanning electron micrographs of the polymer samples was taken on a Cam Scan 2DV unit.

Hydrolytic stability

In order to study the water absorption behavior, the chemically blended silica composite was cut into small pieces. Before testing, the specimens were dried in an oven at 30 ⁰C for 2 h and kept over fused CaCl₂ for 24 h. Then the initial weights (W₁) of the samples were measured. After that these samples were immersed in distilled water and after 7 days of immersion the specimens were taken out and wiped well with filter paper. The swelled weight (W₂) was measured again carefully and water absorption was calculated using the following relation.

$$\% \text{ Water absorption} = [W_2 - W_1] / W_1 \times 100$$

Stability in acid

In order to measure the stability of the composite samples prepared by above mentioned method in acid medium we used 10^{-6} M HCl. Before testing all the prepared specimens were kept over fused CaCl_2 for 24 h followed by measurements of weights (X) of all the samples. Then the specimens were immersed in HCl solution. After definite time of interval specimen were taken out and washed thoroughly with distilled water to remove traces of acid, if any. Then the specimens were dried carefully before measuring the final weight. The final weight of the samples was measured (Y). Any decrease or increase in weight of the glass specimen was calculated by using the following relation. From this value we can know whether any decomposition or any change takes place or not due to the action of acid.

$$\% \text{ Weight loss} = [X - Y] / X \times 100$$

X-Ray diffraction analysis

XRD profiles were recorded on a Philips PW-1840 x-ray diffractometer using $\text{Cu K}\alpha$ radiation of wavelength 0.154 nm. The instrument was operated at 40 KV and 20 mA. The powdered samples were pressed in a square plastic sample holder, which had 1mm deep rectangular hole and pressed against optically smooth glass plate.

Results and Discussion

FTIR and NMR spectroscopic analysis

Infrared spectroscopy has proven to be extremely useful in studies of organic compounds, polymer, organic-inorganic silica glass hybrid, pharmaceuticals and petrochemicals. The characteristics IR bands of the chemically blended silica glass are given in Table 1. FTIR spectrum in the range $400\text{--}4000\text{cm}^{-1}$ has been used as a tool to assign the significant features of the reaction product in comparing them with starting material⁴⁰. The representative set of IR spectra of some selected silica composites are shown in Figure

Table 1 IR spectra of chemically blended silica composite

Characteristics Band	Wave Number (cm^{-1})					
	SiO_2	VNY-SiO_2	Ali-SiO_2	MMA-SiO_2	NAP-SiO_2	Remarks
Si-OH	3741.68	3852.37	3741.30		3763.19	Broad O-H

O-H	3670.78 3531.98 --	--- 3461.65 2357.06	3440.56	3406.45 2361.57 2109.74	3448.04	Hydrogen bonded O-H
C=C str.or the silica over tone band.		1646.93	1644.86	1647.16	1646.74	
C=O str of six membered ring			1541.18		1539.25 1502.58	
C-O str band			1132.56	1384.53		Asymmetric Si-O-C and Si-O-Si absorbs in the same region, with increase in chain length intensity increases.
Si-O-Si and Si-O-C	1070.31	1093.45	1074.56	1073.98	1074.17	
Si-OR		856.26	932.61	742.15 663.83 619.86	862.29 795.53 666.92	

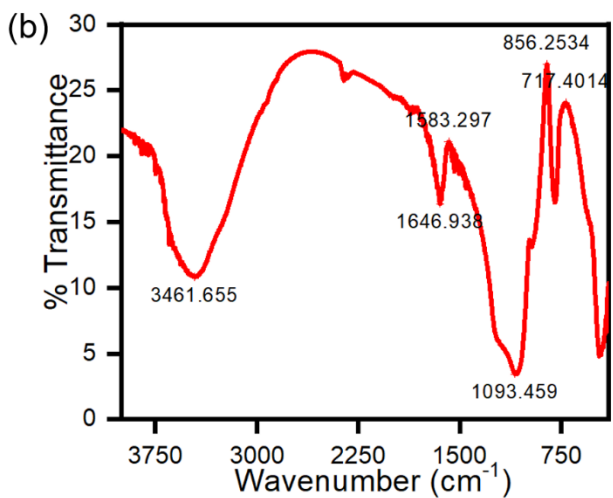
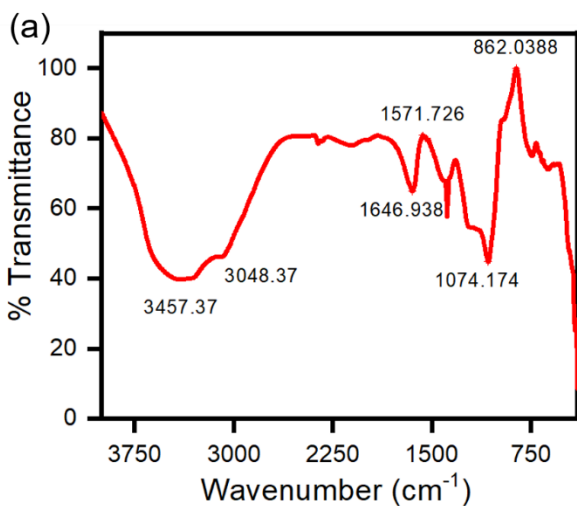
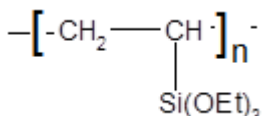
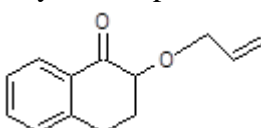
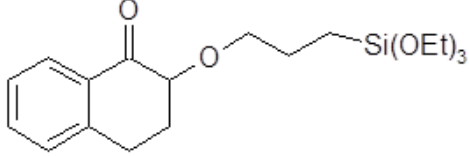
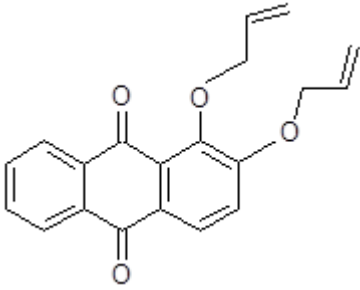
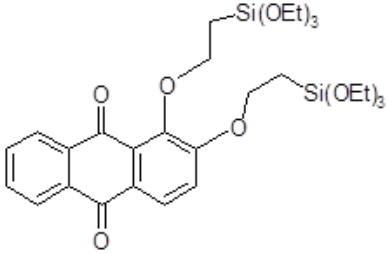


Figure 1. IR spectrum of (a) NAP-SiO₂ composite and (b) VIN-SiO₂ glass

The most significant features of the inorganic component of these silica composites are that the Si-O-Si and Si-O-C bands appeared at their normal positions. The aforementioned stretching bands appeared at 1070.31 cm⁻¹ (SiO₂), 1093.45 cm⁻¹ (PVNY-SiO₂), 1074.56 cm⁻¹ (Ali-SiO₂), 1073.98 cm⁻¹ (MMA-SiO₂), 1074.17 cm⁻¹ (NAP-SiO₂). The strong O-H stretching vibration of Si-OH group absorbs in the same region as that of alcohol, i.e., at 3700-3200 cm⁻¹. The C=C stretching band found at 1644-1647 cm⁻¹ for all the composites except the silica composite made from pure TEOS. The C=O stretching band appeared at 1541.18 cm⁻¹ for ALI-SiO₂ composite and at 1539.53 cm⁻¹ for NAP-SiO₂ composite. However, a comparison of the assignments for each spectrum showed no significant differences.

The NMR characterization data of these compounds is summarized in Table 2

Compound	NMR Characteristics (CDCl ₃ , 200 MHz)
Poly vinyl triethoxy silane 	1.17-1.33 (br t), 3.40-3.85 (br q)
Allylated naphthol 	4.59-4.62 (m, 2H), 5.96-6.12 (m, 1H), 6.18 (s, 1H), 7.66-7.79 (m, 2H), 8.05- 8.15 (m, 2H)
Hydrosilylated naphthol	1.07 (t, 3H), 1.53 (t, 2H) 1.81-1.95 (m, 3x 2H), 3.96 (t, 2H J=6.63 Hz) 4.07 (bq, 3x2H), 6.14 (s, 1H), 7.69-7.74 (m, 2H), 8.04-8.10 (m, 2H)

	
<p>Allylated alizarin</p> 	<p>4.67-4.72 (m, 4H), 5.26-5.51 (m, 4H), 6.04-6.10 (m, 1H), 6.26-6.28(m, 1H), 7.23 (d, 1H, J=5.79), 7.73-7.78 (m, 2H), 8.14(d, 1H, J= 5.78), 8.23-8.28 (m,2H)</p>
<p>Hydrosilylated alizarin</p> 	<p>0.70-1.27(m, 22H), 3.67-3.91(m, 12H), 4.06-4.15(m,4H)7.17 (d,1H, J=8.4) 7.77- 7.84 (m, 2H), 8.29-8.31 (m, 2H)</p>

Thermal analysis

Thermal analysis diagrams, shown in Figures 3a-b and 4 a-d were used to study the thermal stability of the chemically blended silica composites. Thermal analysis diagram had been collected to study the changes of inorganic-organic hybrid glass with thermal treatment. The results are presented in Table 2. Each TGA diagram exhibited three weight loss stages though the onset of decomposition temperature was slightly different from one another.

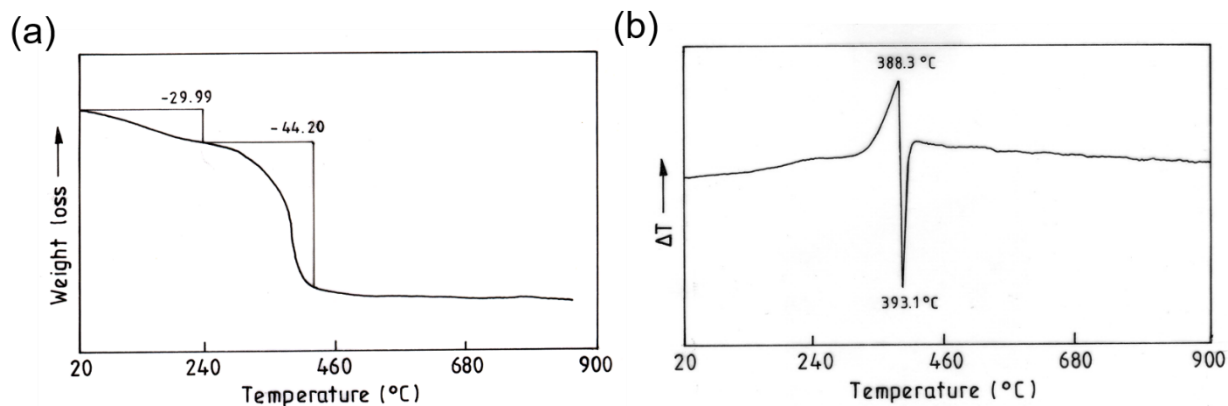


Figure 3(a-b). TGA –DTG diagram of VNY-SiO₂ composite

Table 2 Thermal analysis diagram of chemically blended silica glass

Sample designation	Decomposition temperature (0°C)								
	First stage			Second stage			Third Stage		
	Initial	Final	Mass loss (%)	Initial	Final	Mass loss (%)	Initial	Final	Mass loss (%)
VNY-SiO ₂	30	240	29	240	440	44	440	680	2
MMA-SiO ₂	29	153	8	153	417	36	417	501	1
NAP-SiO ₂	82	130	55	130	710	26	587	997	17
Chem-ALI-SiO ₂	95	200	15	200	587	23	684	990	2
SiO ₂	58	225	18	225	684	28	--	---	---

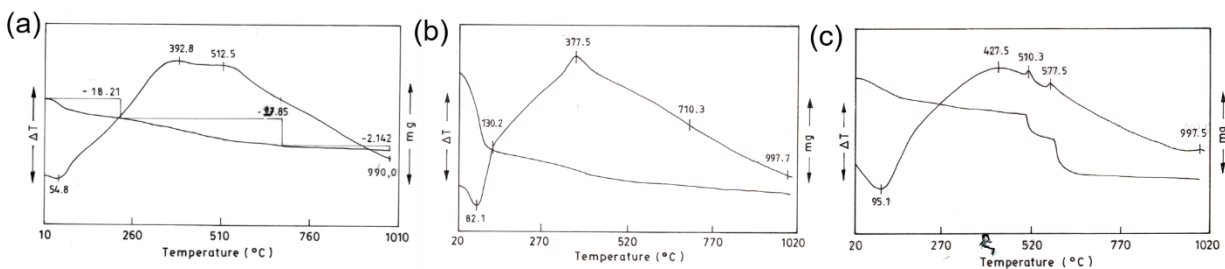


Figure 4 Thermal diagram of (a) SiO₂ glass, (b) NAP-SiO₂ composite and (c) Chem-ALI-SiO₂ composite

The differences could be attributed to the presence of different organic molecules. A gradual weight loss occurred below 250 °C. Mass loss was less than 30% in most of the cases. The weight loss was due to evaporation of water and volatilization and thermal decomposition of the trapped organic solvent. Since in this process gelling and condensation were performed at ambient atmosphere a greater amount of solvent and water molecules got trapped in these composites. It was seen from the TGA profiles of NAP-SiO₂ composite that it exhibited 59% weight loss in the first stage (22.4-130 °C). From the DTG curve a corresponding endothermic peak was observed at 82.1 °C. It might be due to the evaporation of the trapped solvent (THF and ethanol). But in all other cases major weight loss occurred during the second degradation stage. This could be attributed to the thermal decomposition of the organic moiety. DTG curve showed an exothermic peak at this temperature range (150-600 °C). It was believed that exothermic peaks arise due to restructuring during crystallization process and oxidation of the organic matrix^{41, 42}. It was evident that the oxidation of the organic molecules coming from the dye or polymer occurred at higher temperature. Such exothermic peaks were absent in the case of samples prepared without polymer. The location of the peak and their relative position depend on the structural properties of the gel⁴³. In case of alizarin composite the 2-3% weight loss occurred in the final stage of decomposition. After the loss of organic component, the TGA curves became flat up to 900°C with only inorganic material remaining.

Comparison of thermal stability between physically and chemically blended. silica glass.

Table 3 Thermal stability of physically and chemically blended silica glass composites

Sample designation	Decomposition temperature (0° C)								
	First stage			Second stage			Third stage		
	Initial	Final	Mass loss (%)	Initial	Final	Mass loss (%)	Initial	Final	Mass loss (%)
Phy-Ali-SiO ₂	23	112	56	112	645	32	645	997	1

Chem-Ali- SiO ₂	22	200	15	200	587	23	587	997	16
----------------------------	----	-----	----	-----	-----	----	-----	-----	----

We discussed the preparation and properties of physically blended alizarin-silica composites. Here we deal with chemically blended alizarin-silica composites. For these composites we have selected alizarin as one of the starting materials for preparation of both physically and chemically blended silica composites. It has been reported that physically blended alizarin and silica glass disintegrates through crack formation during slow drying of the gel. Although initially a homogenous blend of alizarin in THF and aqueous TEOS was formed but during drying by evaporation of solvents alizarin was separated into a discrete phase apart from disintegration of the glass. Therefore, we thought that if alizarin could be chemically bound to SiO₂ matrix, probably those drawbacks of phase separation and cracking could be overcome. In order to chemically bind alizarin to silica it was first fictionalized through allylation of its hydroxyl group followed by hydrosilylation of the allyl group. Then this functionalized alizarin was simultaneously hydrolyzed and co-condensed with TEOS. Thus, the alizarin molecule becomes chemically bonded through the allyl group to SiO₂ matrix. The sequences of reactions of alizarin and TEOS are shown in Scheme 4. It was well known that acid catalyzed glass formation by hydrolysis of TEOS was a slow process during which time a three-dimensional network of glass was formed with slow evaporation of solvent. In absence of chemical linkage of alizarin to silica a mechanical stress was developed due to shrinkage of glass network by the evaporation of the solvent. As such the silica network was rigid and alizarin also contains two benzene rings fused to an anhydride ring making it highly rigid. Therefore, both alizarin and silica being rigid form a highly amorphous and brittle three-dimensional structure and expulsion of solvent from the swelled hydrogel force the gel network to collapse. On the contrary, when alizarin was chemically linked through a –CH₂-CH₂- bridge to SiO₂ the gel did not collapse and crack after evaporation of solvent. This observation occurred due to the flexible –CH₂-CH₂- linkage that prevented the gel from cracking.

The results of the comparative study with these composites are given in Table.3. It was observed that stability of chemically blended alizarin composite (Chem-Ali- SiO₂) was higher than that of physically blended (Phy-Ali-SiO₂) one. Thermal diagram indicated that both composites exhibited three stages of decomposition. Initial decomposition took place within the temperature region 22⁰C-200⁰C. In case of physically blended (Phy-Ali-SiO₂) silica glass 56.8 % weight loss

has been taken place in the first stage. On the other hand, chemically blended silica composite exhibited 15% weight loss during the initial stage of decomposition. It also indicated greater degree of condensation during the preparation of chemically blended silica glass. During second stage of decomposition both the composites exhibited comparable mass loss. In this stage mass loss occurred due to the decomposition of organic component. Total weight loss in case of former composite was 90.56% whereas for the latter case it was 54.56%. From the result it was clear that chemically blended silica glass exhibited greater thermal stability.

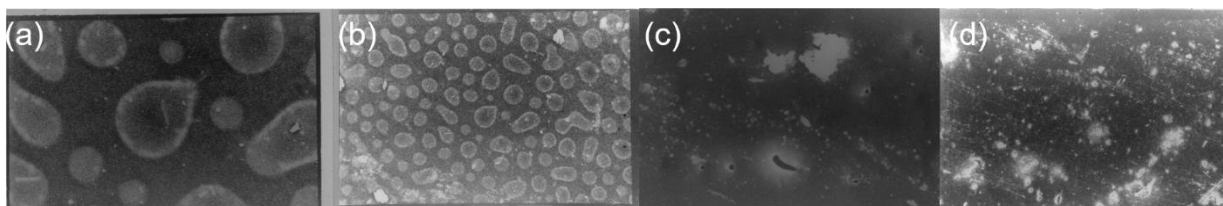


Figure 5 SEM micrographs of (a-b) silica composite, (c) NAP-SiO₂ composite (d) ALI –SiO₂ composite

The scanning electron micrographs revealed some interesting morphological differences between the SiO₂ prepared from TEOS and different chemically blended silica composites. Figure 4a represented SEM micrographs of silica glass prepared from TEOS. Particles of different shapes and sizes are observed in the Figure 5a. Figures 5 (c-d) represented SEM micrographs of chemically blended silica glass hybrids like Nap-SiO₂ and Chem-Ali-SiO₂. It was observed that the particles appeared to be more densely packed with relatively smaller size. It was quite different from that of the Figure 5a. But the general morphological feature of various chemically blended silica composites was not different from one another, non-uniform particle distribution was the conspicuous feature.

Hydrolytic stability

One of the big problems of unmodified SiO₂ gels, in particular for technical use is their long –term stability under humid atmosphere. Owing to large number of silane groups on the inner surface of the material, adsorption and capillary condensation of water may cause cracking of the composite.

Water absorption characteristics of chemically modified silica glass after 7 days immersion in water at room temperature are shown in Figure 6. Comparison of water uptake exhibited that highest water absorption takes place in case of naphthol composite (NAP-SiO₂).

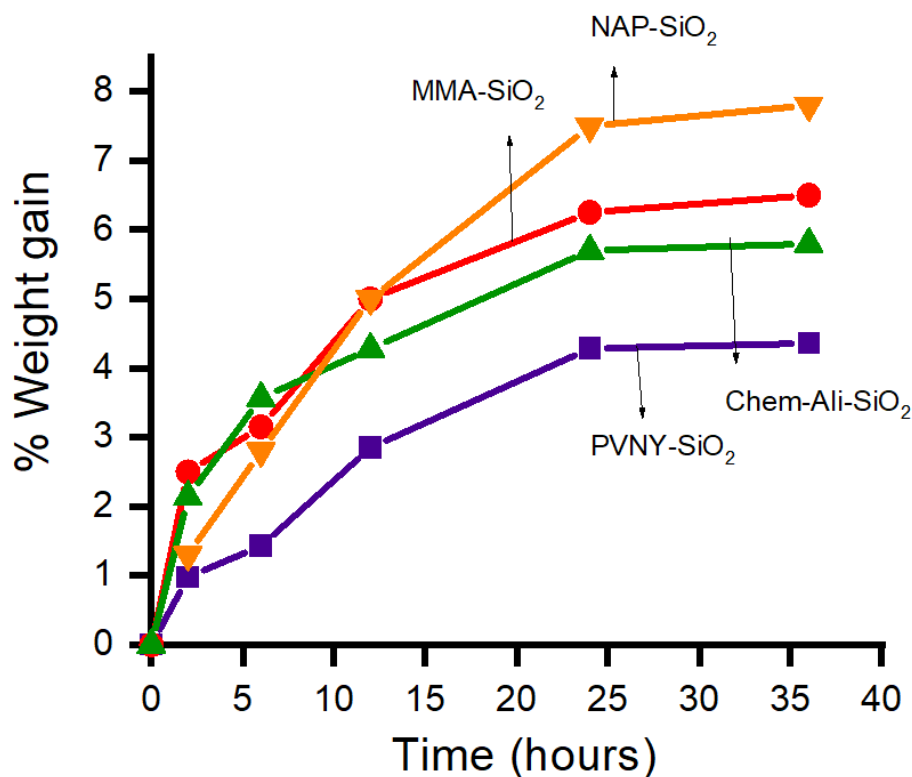


Figure 6. Water absorption studies of chemically blended silica glasses

It is well known that water absorption takes place either by capillary action through void space or by H-bonding with the polar part of the molecule. Hence, with increase in void space or polar functional group water absorption increases. In naphthol-silica composite due to monoallylation less cross-linking occurred, and greater void space may remain in the final hybrid composite. This may be the reason of higher water up take. In MMA-SiO₂ composite besides the void space, polar OCH₃ group may be responsible for water absorption by hydrogen bonding. In chemically blended alizarin composite and PVNY-SiO₂ composite water absorption was quite low due to greater cross linking.

Stability in acid

Table 4 Acid Stability of chemically blended silica glass

Sample	2hr	24 hr	7 days
PVNY-Si	0.0	4.5	4.5
PMMA-Si	0.0	0.0	5.9
NAP-Si	0.0	0.0	0.0
ALI -Si	0.0	0.0	broken

The resistance of prepared chemically blended glasses towards different concentration of mineral acid like HCl was studied. It was observed from Table 4 that weight loss of different composite was negligible in acid medium. But only chemically blended alizarin composite was broken. This was due to breakage of hydrolysable linkage. The good stability of other silica composite in acid medium of was due to non-hydrolysable linkage. This was also an indication of larger degree of polycondensation.

X-Ray diffraction analysis

Microstructure of the porous chemically blended silica composites were investigated by X-Ray diffraction (Figure 7). All the composites are amorphous.

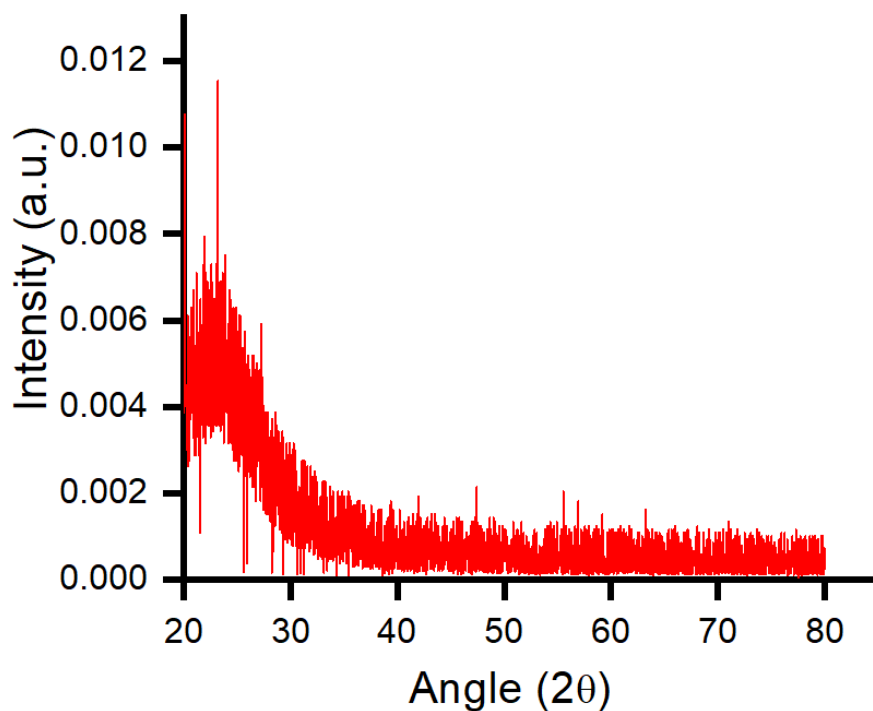


Figure 7. X-Ray diffraction profile of Ali-SiO₂ Composite

Conclusion

We have synthesized chemically blended hybrid glass, in which polymer molecule or monomer molecule are uniformly distributed and covalently bonded to inorganic matrices. We studied all the glass composites by IR, TGA and SEM etc. experiments. All hybrid composites present a good thermal stability, water resistance and good stability in acid solution. It is clear from literature survey that sol-gel processing has huge potential to produce a wide range of specialized products in established composition as well as novel composition not readily accessible by conventional manufacturing techniques.

References

1. Sakka, S.; Kamiya, K., The sol-gel transition in the hydrolysis of metal alkoxides in relation to the formation of glass fibers and films. *Journal of Non-Crystalline Solids* **1982**, 48 (1), 31-46.
2. Ward, D. A.; Ko, E. I., Preparing Catalytic Materials by the Sol-Gel Method. *Industrial & Engineering Chemistry Research* **1995**, 34 (2), 421-433.
3. Mann, S.; Burkett, S. L.; Davis, S. A.; Fowler, C. E.; Mendelson, N. H.; Sims, S. D.; Walsh, D.; Whilton, N. T., Sol-Gel Synthesis of Organized Matter. *Chemistry of Materials* **1997**, 9 (11), 2300-2310.
4. Ray, P.; Ferraro, M.; Haag, R.; Quadir, M., Dendritic Polyglycerol-Derived Nano-Architectures as Delivery Platforms of Gemcitabine for Pancreatic Cancer. *Macromol Biosci* **2019**, 19 (7), e1900073.
5. Ray, P.; Haideri, N.; Haque, I.; Mohammed, O.; Chakraborty, S.; Banerjee, S.; Quadir, M.; Brinker, A. E.; Banerjee, S. K., The Impact of Nanoparticles on the Immune System: A Gray Zone of Nanomedicine. *Journal of Immunological Sciences* **2021**, 5 (1).
6. Ray, P.; Dutta, D.; Haque, I.; Nair, G.; Mohammed, J.; Parmer, M.; Kale, N.; Orr, M.; Jain, P.; Banerjee, S.; Reindl, K. M.; Mallik, S.; Kambhampati, S.; Banerjee, S. K.; Quadir, M.,

pH-Sensitive Nanodrug Carriers for Codelivery of ERK Inhibitor and Gemcitabine Enhance the Inhibition of Tumor Growth in Pancreatic Cancer. *Molecular Pharmaceutics* **2021**, 18 (1), 87-100.

7. Ray, P.; Kale, N.; Quadir, M., New side chain design for pH-responsive block copolymers for drug delivery. *Colloids and Surfaces B: Biointerfaces* **2021**, 200, 111563.

8. Clément, M.; Abdellah, I.; Ray, P.; Martini, C.; Coppel, Y.; Remita, H.; Lampre, I.; Huc, V., Synthesis and NMR study of trimethylphosphine gold(i)-appended calix[8]arenes as precursors of gold nanoparticles. *Inorganic Chemistry Frontiers* **2020**.

9. Abdullah, C. S.; Ray, P.; Alam, S.; Kale, N.; Aishwarya, R.; Morshed, M.; Dutta, D.; Hudziak, C.; Banerjee, S. K.; Mallik, S.; Banerjee, S.; Bhuiyan, M. S.; Quadir, M., Chemical Architecture of Block Copolymers Differentially Abrogate Cardiotoxicity and Maintain the Anticancer Efficacy of Doxorubicin. *Molecular Pharmaceutics* **2020**, 17 (12), 4676-4690.

10. Confeld, M. I.; Mamnoon, B.; Feng, L.; Jensen-Smith, H.; Ray, P.; Froberg, J.; Kim, J.; Hollingsworth, M. A.; Quadir, M.; Choi, Y.; Mallik, S., Targeting the tumor core: hypoxia-responsive nanoparticles for delivery of chemotherapy to pancreatic tumors. *Molecular Pharmaceutics* **2020**.

11. Sarker, N. C.; Ray, P.; Pfau, C.; Kalavacharla, V.; Hossain, K.; Quadir, M., Development of Functional Nanomaterials from Wheat Bran Derived Arabinoxylan for Nucleic Acid Delivery. *Journal of Agricultural and Food Chemistry* **2020**, 68 (15), 4367-4373.

12. Ray, P.; Nair, G.; Ghosh, A.; Banerjee, S.; Golovko, M. Y.; Banerjee, S. K.; Reindl, K. M.; Mallik, S.; Quadir, M., Microenvironment-sensing, nanocarrier-mediated delivery of combination chemotherapy for pancreatic cancer. *Journal of Cell Communication and Signaling* **2019**.

13. Ray, P.; Alhalhooly, L.; Ghosh, A.; Choi, Y.; Banerjee, S.; Mallik, S.; Banerjee, S.; Quadir, M., Size-Transformable, Multifunctional Nanoparticles from Hyperbranched Polymers for Environment-Specific Therapeutic Delivery. *ACS Biomaterials Science & Engineering* **2019**, 5 (3), 1354-1365.

14. Ray, P.; Clément, M.; Martini, C.; Abdellah, I.; Beaunier, P.; Rodriguez-Lopez, J.-L.; Huc, V.; Remita, H.; Lampre, I., Stabilisation of small mono- and bimetallic gold-silver nanoparticles using calix[8]arene derivatives. *New Journal of Chemistry* **2018**, 42 (17), 14128-14137.

15. Ray, P.; Confeld, M.; Borowicz, P.; Wang, T.; Mallik, S.; Quadir, M., PEG-b-poly (carbonate)-derived nanocarrier platform with pH-responsive properties for pancreatic cancer combination therapy. *Colloids Surf B Biointerfaces* **2018**, 174, 126-135.

16. Jayanta, R.; Leena, B., *Preparation and Evaluation of Novel Bamboo-Polymer Composites*. 2021.

17. Ray, P.; Gidley, D.; Badding, J. V.; Lueking, A. D., UV and chemical modifications of polymer of Intrinsic Microporosity 1 to develop vibrational spectroscopic probes of surface chemistry and porosity. *Microporous and Mesoporous Materials* **2019**, 277, 29-35.

18. Ray, J. K.; Singha, R.; Ray, D.; Ray, P.; Rao, D. Y.; Anoop, A., Palladium-catalyzed expedient Heck annulations in 1-bromo-1,5-dien-3-ols: Exceptional formation of fused bicycles. *Tetrahedron Letters* **2019**, 60 (13), 931-935.

19. Ray, P.; Xu, E.; Crespi, V. H.; Badding, J. V.; Lueking, A. D., In situ vibrational spectroscopy of adsorbed nitrogen in porous carbon materials. *Physical Chemistry Chemical Physics* **2018**, 20 (22), 15411-15418.

20. Ray, J. K.; Paul, S.; Ray, P.; Singha, R.; Rao, D. Y.; Nandi, S.; Anoop, A., Pd-catalyzed intramolecular sequential Heck cyclization and oxidation reactions: a facile pathway for the

synthesis of substituted cycloheptenone evaluated using computational studies. *New Journal of Chemistry* **2017**, 41 (1), 278-284.

21. Chaudhuri, S.; Maity, S.; Roy, M.; Ray, P.; Ray, J. K., A Vinyl Radical Cyclization Route to Hydroxycyclohexene Fused Carbocycles. *Asian Journal of Chemistry* **2016**, 28 (1).
22. Ray, P.; Gray, J. L.; Badding, J. V.; Lueking, A. D., High-Pressure Reactivity of Triptycene Probed by Raman Spectroscopy. *The Journal of Physical Chemistry B* **2016**, 120 (42), 11035-11042.
23. Ray, P., Interactions of nitrogen and hydrogen with various 1D and 3D carbon materials probed via in-situ vibrational spectroscopy. *Ph. D. Thesis* **2016**.
24. Wang, C.-Y.; Ray, P.; Gong, Q.; Zhao, Y.; Li, J.; Lueking, A. D., Influence of gas packing and orientation on FTIR activity for CO chemisorption to the Cu paddlewheel. *Physical Chemistry Chemical Physics* **2015**, 17 (40), 26766-26776.
25. Brahma, S.; Ray, P.; Singha, R.; Ray, J. K., Visible Colourimetric and Ratiometric Fluorescent Chemosensors for Cu (II) and Ni (II) Ions. *Asian Journal of Chemistry* **2016**, 28 (5), 1035.
26. Singha, R.; Roy, S.; Nandi, S.; Ray, P.; Ray, J. K., Palladium-catalyzed one-pot Suzuki–Miyaura cross coupling followed by oxidative lactonization: a novel and efficient route for the one-pot synthesis of benzo[c]chromene-6-ones. *Tetrahedron Letters* **2013**, 54 (7), 657-660.
27. Ray, D.; Nasima, Y.; Sajal, M. K.; Ray, P.; Urinda, S.; Anoop, A.; Ray, J. K., Palladium-Catalyzed Intramolecular Oxidative Heck Cyclization and Its Application toward a Synthesis of (\pm)- β -Cuparenone Derivatives Supported by Computational Studies. *Synthesis* **2013**, 45 (09), 1261-1269.
28. André, E.; Boutonnet, B.; Charles, P.; Martini, C.; Aguiar-Hualde, J. M.; Latil, S.; Guérineau, V.; Hammad, K.; Ray, P.; Guillot, R.; Huc, V., A New, Simple and Versatile Strategy for the Synthesis of Short Segments of Zigzag-Type Carbon Nanotubes. *Chemistry* **2016**, 22 (9), 3105-14.
29. Parkhurst, C. S.; Doyle, W. F.; Silverman, L. A.; Singh, S.; Andersen, M. P.; McClurg, D.; Wnek, G. E.; Uhlmann, D. R., Siloxane Modified SiO₂-TiO₂ Glasses via Sol-Gel. *MRS Online Proceedings Library* **1986**, 73 (1), 769-773.
30. Bates, F. S., Block copolymers near the microphase separation transition. 2. Linear dynamic mechanical properties. *Macromolecules* **1984**, 17 (12), 2607-2613.
31. Glaser, R. H.; Wilkes, G. L., Structure property behavior of polydimethylsiloxane and poly(tetramethylene oxide) modified TEOS based sol-gel materials. *Polymer Bulletin* **1988**, 19 (1), 51-57.
32. Lebeau, B.; Sanchez, C., Sol-gel derived hybrid inorganic-organic nanocomposites for optics. *Current Opinion in Solid State and Materials Science* **1999**, 4 (1), 11-23.
33. Wang, B.; Wilkes, G. L.; Hedrick, J. C.; Liptak, S. C.; McGrath, J. E., New high-refractive-index organic/inorganic hybrid materials from sol-gel processing. *Macromolecules* **1991**, 24 (11), 3449-3450.
34. Calvert, P., Vegetable and mineral. *Nature* **1991**, 353 (6344), 501-502.
35. Pope, E. J. A.; Asami, M.; Mackenzie, J. D., Transparent silica gel–PMMA composites. *Journal of Materials Research* **1989**, 4 (4), 1018-1026.
36. Schmidt, H., Organic modification of glass structure new glasses or new polymers? *Journal of Non-Crystalline Solids* **1989**, 112 (1), 419-423.

37. Tsumura, M.; Ando, K.; Kotani, J.; Hiraishi, M.; Iwahara, T., Silicon-Based Interpenetrating Polymer Networks (IPNs): Synthesis and Properties. *Macromolecules* **1998**, *31* (9), 2716-2723.
38. Novak, B. M.; Davies, C., "Inverse" organic-inorganic composite materials. 2. Free-radical routes into nonshrinking sol-gel composites. *Macromolecules* **1991**, *24* (19), 5481-5483.
39. Yen, W.; Dachuan, Y.; Bakthavatchalam, R., Thermal stability and hardness of new polyacrylate-SiO₂ hybrid sol-gel materials. *Materials Letters* **1992**, *13* (4), 261-266.
40. Ebdon, J. R., Principles of polymerization George Odian John Wiley and Sons, Inc., New York, 1991. pp. 768, price E47.50. ISBN 0-471-61020-8. *Polymer International* **1993**, *30* (2), 281-281.
41. Lenz, R. W., Experiments in polymer science, Edward A. Collins, Jan Bares, Fred W. Billmeyer, Jr., Wiley-Interscience, New York, 1973. 530 pp. \$16.95. *Journal of Polymer Science: Polymer Letters Edition* **1974**, *12* (9), 535-536.
42. Colby, M. W.; Osaka, A.; Mackenzie, J. D., Effects of temperature on formation of silica gel. *Journal of Non-Crystalline Solids* **1986**, *82* (1), 37-41.
43. Pauthe, M.; Phalippou, J.; Corriu, R.; Leclercq, D.; Vioux, A., Silica xerogels containing a functional group at silicon. *Journal of Non-Crystalline Solids* **1989**, *113* (1), 21-30.